Materials Science in Semiconductor Processing 28 (2014) 115–120

Contents lists available at ScienceDirect

Materials Science in Semiconductor Processing

journal homepage: www.elsevier.com/locate/mssp

Modeling of sub-band and diameter effect in carrier concentration of CNTFET

Abdelmalek Mouatsi *, Mimia Marir-Benabbas

Laboratory of Modeling Devices Energy Renewable and Nanometric (MoDERNa), Department of Electronic, University of Constantine 1, Constantine, Algeria

ARTICLE INFO

Available online 17 August 2014

Keywords:
Carrier concentration
Band structure
Carbon nanotube diameter
CNTFET
Zone folding

ABSTRACT

Carbon nanotubes (CNTs) have been seen as a potentially future material to provide an ultrasmall device (CNTFET (Carbon Nanotube Field Effect Transistor)). Therefore, the studies of sub-bands effects are needed in order to find the enhancement of carrier transport in CNTFET.

Also in this paper the band structure of the rolled-up nanotube can be obtained by zone-folding from the band structure of the graphene sheet. This method is used in this work and we simulated and analyzed the band structure of carbon nanotube. We present analytical modeling of carrier concentration in a zigzag semiconducting of carbon nanotube field effect transistor (CNFET) using the dispersion relation $E(k)$ (the first three sub-bands) and given the density of states (DOS), the carrier concentration is obtained based on a numerical method as an alternative to the usual Fermi–Dirac integrals. In order to find the influence of the first three sub-bands energy and diameter d_t of CNT in non-degenerate and degenerate region of the carrier concentration in CNTFET. The results obtained showed that the diameter and the energy of sub-band have a significant impact on the carrier concentration of CNTFET.

© 2014 Elsevier Ltd. All rights reserved.

1. Introduction

Carbon nanotubes (CNTs) are one of the most nanomaterials, present exceptional physical, electrical and mechanical properties such as high current density, large mechanical stiffness, and field emission characteristics, which make them the ultimate materials in a wide range of hi-tech applications [1,2].

Since the discovery of CNTs by Iijima in 1991 [3], significant progress has been achieved in both understanding the fundamental properties and exploring possible engineering applications. Carbon nanotubes (CNTs) are hollow cylinders composed of carbon atoms arranged in a hexagonal network with diameters ranging from 1–10 nm, and with lengths up to several micrometers. It can be classified into SWCNT (Single Walled Carbon Nanotube) and MWCNT (Multi Walled Carbon Nanotube) [4,5].

The possible applications in nanometer scale electronics devices have been extensively explored since the demonstration of the first CNT field effect transistors (CNTFETs) [5]. Carbon nanotube field effect transistors (CNTFETs) utilize a semiconducting CNT as channel between two electrodes which work as the source and drain of the transistor, controlled by an isolated electrostatic gate. The structure of a CNT-FET is similar to the structure of a typical MOSFET [6]. When an electric field is applied to a CNT transistor, a mobile charge is induced in the tube from the source and drain.

Several researchers have conducted numerous studies to attempt to model the CNTFET at the end to simulate their

* Corresponding author.
E-mail address: abdelmalek.mouatsi@yahoo.fr (A. Mouatsi).

http://dx.doi.org/10.1016/j.mssp.2014.07.033
1369-8001/© 2014 Elsevier Ltd. All rights reserved.

electrical performance based on physical characteristics of CNT [6,7]. In fact, to foretell the functionality of a CNTFET in electronic devices, the I_{ON} current of CNTFET is limited by the amount of charges introduced into the channel by the gate. We need to know more about the electrical properties, with which calculated carrier concentration (electron or holes) can propagate through the length of the device [6].

In this work, we have studied and analyzed the physical and electrical properties of carbon nanotubes using the zone folding approximation for determining the dispersion energy $E(k)$, and simulated the band structure of CNT with the first three sub-bands energy. We have used the Fermi–Dirac integrals, density of states (DOS) and energy band structure of carbon nanotubes to derive analytical solutions for calculating the carrier concentration. The carrier concentration is obtained based on numerical methods used in order to find the influence of the first three sub-bands energy and diameter in non-degenerate and degenerate region of the carrier concentration in CNTFET.

2. Carbon Nanotube Band Structure

The structure of CNT can be seen as the result of the rolling up of a graphene sheet into a cylinder as shown in Fig. 1. Depending on the orientation of rolling up that is geometrically characterized by the indices n and m which specify the chilarity vector $\vec{C}$ and the diameter d_t of the CNT and determine its fundamental properties [7,8], where

$$\vec{C}=n\vec{a}_1+m\vec{a}_2 \tag{1}$$

$$d_t=(\sqrt{3}a\sqrt{m^2+mn+n^2})/\pi \tag{2}$$

$$\vec{a}_1=a(\sqrt{3}/2,1/2),\quad \vec{a}_2=a(\sqrt{3}/2,-1/2)$$

here $\vec{a}_1$ and $\vec{a}_2$ are lattice unit vectors, and $a=\sqrt{3}a_{C-C}$ (a_{c-c}=0.142 nm is the distance between two carbon atoms).

The properties of the CNT depend on the roll-up direction: when $(n-m)$ is a multiple of 3 the CNT exhibits metallic properties, otherwise it behaves like a semiconductor [9]. The band structure of a SWCNT can be understood in terms of the band structure of graphene; the $E(k)$ values for graphene given in Eq. (3) can be obtained from the tight-binding model given by [10]

$$E_{2D}=\mp\gamma_0[1+4\cos(\sqrt{3}k_xa/2)\cos(k_ya/2)+4\cos^2(k_ya/2)]^{1/2} \tag{3}$$

where $\gamma_0\approx 2.7$ (eV) is the nearest neighbor C–C tight binding overlaps energy and $k_{x,y}$ is wave vector component. Once a graphene is rolled up into a CNT, the boundary conditions imposed by the real physical structure of a CNT along the circumference of the nanotube can be expressed as [10,11]

$$\vec{k}\times\vec{c}_h=2\pi q \tag{4}$$

where $q=0, 1, 2,\ldots N-1$ is the number of carbon pairs in the unit cell

$$N=2(n^2+m^2+nm)/d_R,\quad \text{with } d_R=gcd(2m+n,\ 2n+m).$$

Therefore, the allowed values of k lie on N equidistant lines parallel to the tube axis (Fig. 2) [11].

The one-dimensional (1D) band structure of a (n, m) nanotube is given by the zone-folding relation by using the relation [12]

$$E_{NT}(k,q)=E_{2D}\left(k\frac{K_2}{|K_2|}+qK_1\right) \tag{5}$$

$$K_1=(-t_2b_1+t_2b_2)/N \text{ and } K_2=(mb_1-mb_2)/N.$$

$$t_1=(2m+n)/N \text{ and } t_2=-(2n+m)/N,$$

where

$$b_1=b(1/2,3/2),\quad b_2=b(1/2,-3/2),\quad b=4\pi/3a_{c-c}.$$

3. The Carrier Concentration Modeling

Carrier concentration is an essential parameter for semiconductor. There are two types of carrier concentration to be measured in order to assess the sub-band effects. The carrier concentration is said to be non-degenerate when carrier concentration is lower because there is no interaction between donors or between acceptors. Degenerate is when the carrier is higher because interaction may occur between donors and between acceptors [13]. We assumed thermal equilibrium condition, the total carrier concentration in a band can be

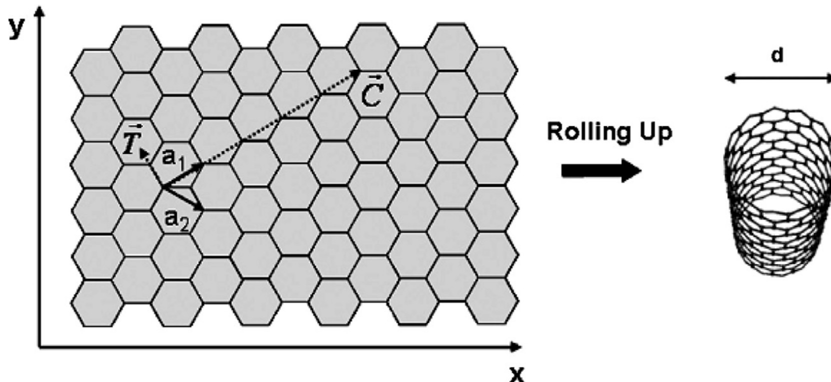

Fig. 1. Structure of a CNT [8].

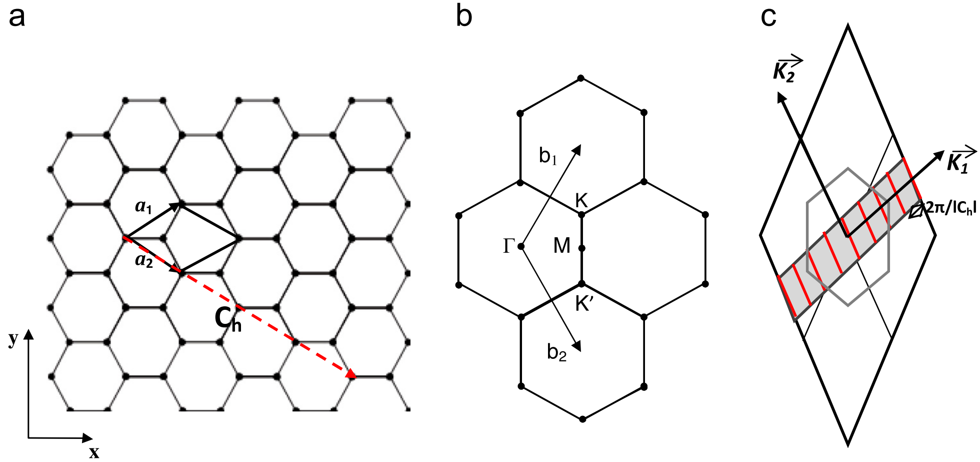

Fig. 2. Brillouin zone and reciprocal space, (a) basis vector in the hexagonal lattice of graphene, (b) Brillouin zone corresponding reciprocal basis vectors $\vec{b}_1$ and $\vec{b}_2$, and (c) the allowed values of k lie on N equidistant lines parallel to the tube axis [11].

estimated from the DOS and Fermi function as [13,14]

$$n = \int_{E_C}^{\infty} \mathrm{DOS}(E) f(E)\, dE \tag{6}$$

where DOS(E) is the density of states, $f(E)$ is the Fermi function, and E_C is the conduction band edge. The DOS(E) equation can be obtained by substituting the equation of $dk=(2\pi/L_x)dN$ [14] for the derivation of the band structure equation $E(k)$ given by the zone folding in Eq. (13). The result of derivation for the DOS per unit length along the axis of CNT semiconductor written as

$$\mathrm{DOS}(E) = dN/L_x dE = \frac{\beta}{2\pi\sqrt{E_g}}(E - E_g/2)^{-1/2} \tag{7}$$

By substituting the density of state DOS(E) and Fermi–Dirac distribution function $f(E)$ expressions into the above formula, the carrier concentration can be evaluated for

$$n = \int_{E}^{\infty} \left[(\beta/2\pi\sqrt{E_g})(E-(E_g/2))^{-1/2}(1/1+e^{((E-E_F)/k_BT)})\right] dE \tag{8}$$

We can rewrite Eq. (8) as

$$n = \left(\beta\sqrt{k_BT}/2\pi\sqrt{E_g}\right) \int_{E}^{\infty} \left(X^{-1/2}/(1+e^{X-\eta})\right) dX, \tag{9}$$

where

$X=(E-(E_g/2))/k_BT$, $\eta=(E_F-(E_g/2))/k_BT$ and $dX/dE=1/k_BT$

k_B is the Boltzmann constant, T is the temperature, and β is a parameter consists of the number of sub-band (used in Eq. (14)). It means, every sub-band will have their own value of β. These equations can be done analytically by using Fermi Dirac integral, the Fermi Dirac integral of order "i" is defined as [15,16]

$$\Im_i = (1/\Gamma(i+1)) \int_0^{\infty} [X^i/(1+e^{X-\eta})] dX \tag{10}$$

By using the Fermi Dirac integral of order $i=-1/2$

$$\Im_{-1/2} = (1/\Gamma((-1/2)+1)) \int_0^{\infty} [X^{-1/2}/(1+e^{X-\eta})] dX \tag{11}$$

Γ is called gamma function, and $\Gamma(1/2)=\sqrt{\pi}$.

Eq. (8) can be written as

$$n = \left(\beta\sqrt{k_BT}/2\sqrt{\pi E_g}\right)\Im_{-1/2} \tag{12}$$

4. Results and discussion

The electronic band structure and carrier concentration of the CNT are important as they provide a better understanding of the electrical properties of CNTFET. The band structure consists of the valence band, band gap and conduction band. Both valence band and conduction band will split into first, second and third sub-bands. The band structure can be simulated when energy-wave vector $E(k)$ dispersion equation is found. Due to the approximation of the graphene band structure and using the zone folding approximation in Eq. (5), the dispersion relation $E(k)$ is [19]

$$E(k,q) \cong \pm \frac{\sqrt{3}a\gamma_0}{2}\sqrt{[(2/d_t)^2(q\pm(1/3))^2]+k^2} \tag{13}$$

$$E(k,q) \cong \pm \frac{E_g}{2}\sqrt{[1+(k^2/\beta^2)]} \tag{14}$$

where

$E_g=\sqrt{3}a\gamma_0\beta$, $\beta=(2/d_t)(q\pm(1/3))$, $d_t=(\sqrt{3}a\sqrt{m^2+mn+n^2})/\pi$,

where E_g is the band gap energy, d_t is the tube diameter, γ_0 is the energy between carbon atom, and a is the lattice constant of the honeycomb network, $a=\sqrt{3}a_{c-c}$ (a_{c-c}= 1.42 Å is the distance between two carbon atoms). The integer variable q counts the available bands, where k is the part of the wave vector that continuously describes the states within a given sub-band (and associated with the direction parallel to the tube axis) [20].

Show in Fig. 3, the graphs of $E(k)$ dispersion based on Eq. (13), and these curves are plotted for CNT semiconductor type zigzag with diameter d_t=0.55 nm and several sub-bands. Based on Fig. 3, the first sub-band has a small band gap, followed by second sub-band and the third sub-band which has the greatest band gap. This indicates that

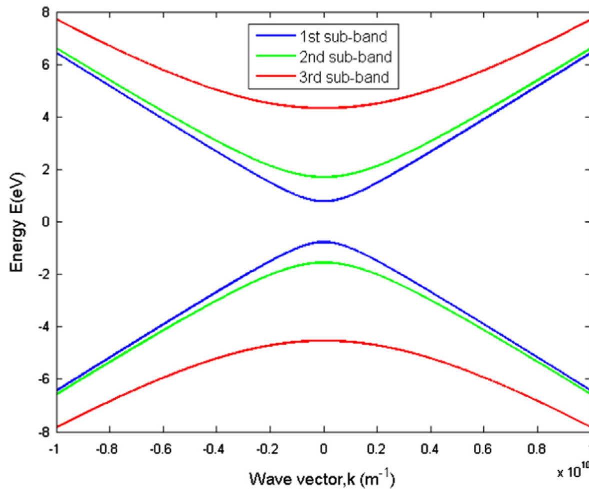

Fig. 3. The dispersion energy $E\ (k)$ with CNT sub-band [19,20].

the carriers in the first sub-band are easier to move from valence to conduction band due to the smaller band gap compared to the other sub-bands. However, when the diameter increased, the band gap for the first, second and third sub-bands becomes too close and the passage of carrier becomes important [19].

Before the effect of sub-band on the carrier concentration, which indicates the number of occupied levels in the band energy per unit length, given in Eq. (12), the non-degenerate and degenerate concentration must be analyzed first.

In non-degenerate region (where $E-E_F \gg 3k_BT$), the Maxwell–Boltzmann approximation is valid, where in this condition [16], $f(E)=e^{E_F-E/k_BT}$ and $\Im_i=e^{\eta}$. Therefore, Eq. (12) will be

$$n=\left(\beta\sqrt{k_BT}/2\sqrt{\pi E_g}\right)e^{\eta} \tag{15}$$

For the degenerate region, the Boltzmann approximation is no longer valid, at this condition [16], $f(E)=1$ and $\Im_{-1/2}=(2/\sqrt{\pi})\eta^{1/2}$; therefore, Eq. (12) will be

$$n=\left(\beta\sqrt{k_BT}/\pi\sqrt{E_g}\right)\eta^{1/2} \tag{16}$$

In general case, $\Im_i$ integration over all conduction band states is required to obtain the total concentration. The upper limit of integration is the top of the conduction band and can be extended to infinity. The Fermi–Dirac integral of Eq. (10) exists for negative orders of $i=(-1/2)$ and the Fermi–Dirac integrals have the property that the derivative of the Fermi–Dirac integral of integer order "i" can be expressed as a Fermi–Dirac integral of order $(i-1)$ where

$$\left(\frac{\partial \Im_i(\eta)}{\partial \eta}\right)=\Im_{i-1}(\eta) \tag{17}$$

The Fermi–Dirac integral of order $i=(-1/2)$ can only be obtained by numerical integration employing Taylor series expansion or by approximate solutions discussed in [16–18].

The curve shown in Fig. 4 represents the non-degenerate and degenerate concentration together with general carrier concentration for the first sub-band. Carrier concentration is proportional to η (eta), which is the variable of the Fermi Dirac integral equation as can be seen in Eqs. (15) and (16). We can see in Fig. 4, in general, the concentrations exponentially increase with increasing η, where Fermi equation has changed and the concentration is linearly proportional to η due to mathematical computation (Eq. (15)).

The formulas for the carrier in non-degenerate region for Eq. (15) have essentially dependence on band gap, temperature, and Fermi energy. We can see that the temperature effects are notable and the thermal effect becomes important in CNTFET characteristic. When the temperature increases, some electrons are thermally excited from the valence band to the conduction band, increasing the electrical conductivity of CNTFET, because the electrical conductivity is proportional to the carrier concentration.

But in degenerate region the Fermi equation is equal to 1 and the formulas for the degenerate carrier for CNTs (Eq. (16)) show that the carrier concentration was independent of temperature and was a strong function of Fermi energy and the band gap energy. The concentrations are exponentially increasing with increasing η.

Based on this simulation, it is shown that when carrier concentration is less than $n\approx 10^7\ \mathrm{m}^{-1}$, the general concentration tends to be in non-degenerate region, while for the concentration exceeds than $n\approx 10^7\ \mathrm{m}^{-1}$, the general concentration starts to be in degenerate region.

The induced carrier from all effective sub-bands in FET devices is an important aspect to determine the output characteristics. In terms of relations between carrier concentration and sub-bands, based in Fig. 5, the carrier concentration for the second and third sub-bands also increase proportionally to η like in the first sub-band.

The carrier concentration in general, degenerate and non-degenerate region is proportional to β (beta), while β is proportional to the number "q" of the sub-band (β of the first sub-band ($q=0$) is small than β of the third sub-bands). Guo et al. [21] have shown that up to two sub-bands are important in determining charge transport in practical CNT transistors.

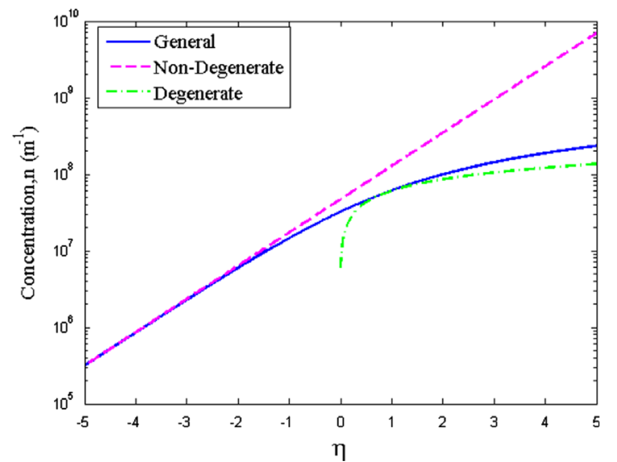

Fig. 4. Carrier concentration versus η for the first sub-band.

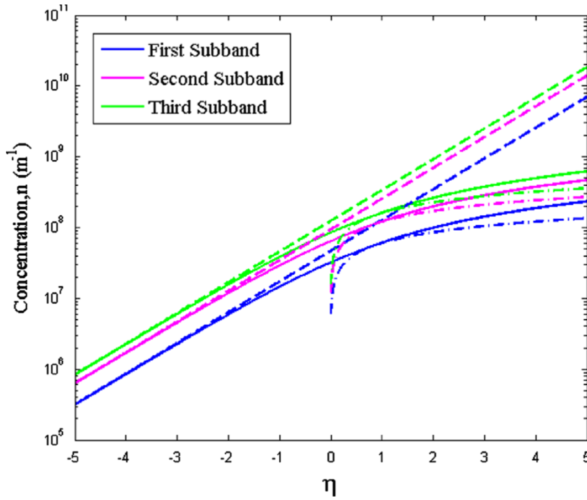

Fig. 5. Carrier concentration versus η for the three first sub-bands.

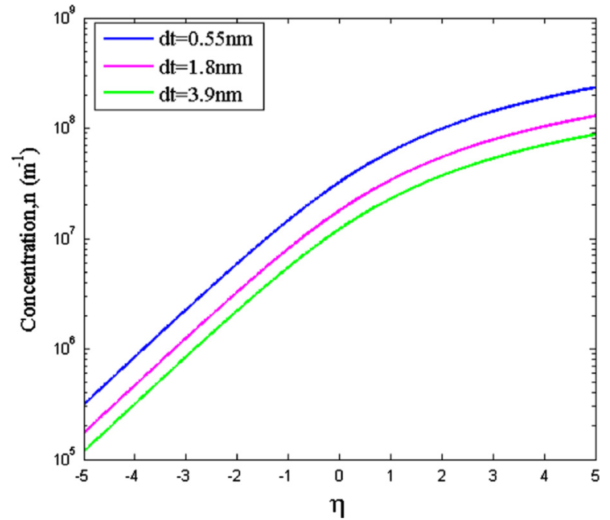

Fig. 6. General carrier concentration versus η for three different CNT diameters.

Moreover, when an electric potential is applied to the gate electrode, the nanotube energy levels are pushed down and the mobile charges are induced in the device [19–21]. Therefore more sub-bands will be participated in the drain current calculation and consequently the saturation drain current will be increased when more carriers are found on the higher bands. But the probability that the higher sub-bands can participated in the drain current calculation is very weak since the energy separation with the other sub-bands is large (of the order of the electron volt).

Based on this simulation, it is shown that when carrier concentration for the first sub-band is $n \approx 10^7\ \mathrm{m}^{-1}$, the general concentration tends to be in non-degenerate region, but in the third sub-bands, the general concentration tends to be in non-degenerate region when carrier concentration $n > 10^7\ \mathrm{m}^{-1}$. This mean, as sub-band goes higher energy gap (E_g) increases and the carrier concentration increases from lower to higher sub-bands.

The diameter d_t of the CNT determines fundamental properties of CNTFET, because CNT used like a channel in CNTFET. From E_g relation we can see that the band gap of semiconducting tubes is inversely proportional to the diameter d_t of CNT. CNT diameter has a first order impact on the drain current value of CNTFET. The increase of the drain current with respect to the diameter is directly associated with the decrease of the CNT band gap energy E_g with its diameter. If the diameters of CNT increase, the band gap E_g becomes small and the separation energy between the seconds and third sub-bands decreases [19].

Fig. 6 presents the general carrier concentration for three different CNT diameters. Based on Fig. 6, it is shown that the general carrier concentration reduced when the diameters of CNT increased, because the carrier concentration is proportional to β (beta), and β is inversely proportional to the diameter. The carrier concentration is important if the diameter is large, because the band gap E_g becomes small and the CNT tends to behave as metallic (more carriers are found on the higher bands). But at the smaller diameter the probabilities that the higher sub-bands will be occupied are typically neglected because the band gap becomes large and the energy separation between sub-bands is large.

5. Conclusion

The electronic transport properties of CNTFET have been widely explored during the last decade. Previous works in carbon nanotubes describing a relationship between the dispersion of energy $E(k)$ and the carbon nanotube sub-bands, this calculation obtained from a zone-folding method. We have derived an analytical method for calculating the carrier concentration for semiconducting CNTs zigzag based on the dispersion of energy $E(k)$ and the Fermi–Dirac distribution function.

The simulation result is explained; first, modeling of the band structure shows that the first sub-band has a lower band gap and the third sub-band exhibits a biggest band gap.

Next, the modeling discussed that the carrier concentration in general is proportional to the sub-band and the carrier concentration increases from lower to the higher sub-band. The lowest energy bands play the greatest role in determining CNTFET characteristic behavior as they are the most to be occupied and the most to be used for carrier movement. The diameter has a significant impact on the carrier concentration of CNTFET.

References

[1] Hervet Fanet, Micro et nanoélectronique: Bases–Composants–Circuits, Dunod, Paris, 2006.
[2] B.E. Joshua, J.D. Andrew, Nanofluidics: Nanoscience and Nanotechnology, Imperial College London, London, 2009.
[3] S. Iijima, Nature 354 (1991) 56–58.
[4] S. Iijima, T. Ichihashi, Nature 363 (1993) 603–605.
[5] Jien Cao, Qian Wang, Hongjie Dai, Phys. Rev. Lett. 90 (2003) 157–601.
[6] P.R. Bandaru, J. Nanosci. Nanotechnol. 7 (2007) 1–29.
[7] J. Appenzeller, J. Knoch, R. Martel, V. Derycke, S.J. Wind, P. Avouris, IEEE Trans. Nanotechnol. 1 (2002) 184–189.

[8] Xu Zhao, Yan Wang, Zhi-Ping Yu, Chin. Phys. Lett. 23 (2006) 1327–1330.
[9] M.A. Grado-Caffaro, M. Grado-Caffaro, Optik 116 (2005) 459–460.
[10] P.A. Alvi, K.M. Lal, M.J. Siddiqui, S. Alim, H. Naqvi, Indian J. Pure Appl. Phys. 43 (2005) 899–904.
[11] L. Xinghui, Z. Changchuna, L. Yukui, Physica B 344 (2003) 243–248.
[12] Tsung-Lung Lia, Jyh-Hua Ting, Physica B 393 (2006) 195–203.
[13] Donald A. Neamen, Semiconductor Physics and Devices: Basic Principles, 3rd edition, McGraw Hill Higher Education International Edition, New York, 2003.
[14] J.W. Mintmire, C.T. White, Phys. Rev. Lett. 81 (1998) 2506–2509.
[15] Muhammad Taher Abuelma'atti, Solid-State Electron. 37 (1994) 1367–1369.
[16] J.S. Blakemore, Solid-State Electron. 25 (1982) 1067–1076.
[17] Frank G. Lether, J. Sci. Comput. 15 (2000) 479–497.
[18] P. Van Halen, D.L. Pulfrey, J. Appl. Phys. 57 (1985) 5271–5274.
[19] A. Mouatsi, M. Marir-Benabbas, H. Baudrand, Int. Rev. Phys. 6 (2012) 68–72.
[20] A. Mouatsi, M. Marir-Benabbas, H. Baudrand, in: Proceedings of the IEEE Conference Publications (SETIT), 2012, pp. 166–170.
[21] J. Guo, A. Javey, H. Dai and M. Lundstrom, in: Proceedings of IEEE IEDM Technical Digest, 2004, pp. 703–706.